Electron scattering in helium for Monte Carlo simulations

Alexander V. Khrabrov and Igor D. Kaganovich

Citation: Physics of Plasmas (1994-present) **19**, 093511 (2012); doi: 10.1063/1.4751865
View online: http://dx.doi.org/10.1063/1.4751865
View Table of Contents: http://scitation.aip.org/content/aip/journal/pop/19/9?ver=pdfcov
Published by the AIP Publishing

Electron scattering in helium for Monte Carlo simulations

Alexander V. Khrabrov and Igor D. Kaganovich
Princeton Plasma Physics Laboratory, Princeton, New Jersey 08543, USA

(Received 26 April 2012; accepted 19 July 2012; published online 26 September 2012)

An analytical approximation for differential cross-section of electron scattering on helium atoms is introduced. It is intended for Monte Carlo simulations, which, instead of angular distributions based on experimental data (or on first-principle calculations), usually rely on approximations that are accurate yet numerically efficient. The approximation is based on the screened-Coulomb differential cross-section with energy-dependent screening. For helium, a two-pole approximation of the screening parameter is found to be highly accurate over a wide range of energies. © *2012 American Institute of Physics*. [http://dx.doi.org/10.1063/1.4751865]

I. INTRODUCTION

Accurate representation of anisotropic scattering in collisions is required for particle simulations of plasmas with energetic (10^2-10^3 eV) electrons, especially in weakly collisional regimes. A high-voltage glow discharge in helium is a good example. To simulate the discharge kinetics, defined by nonlocal transport and non-Maxwellian velocity distributions, one needs to correctly represent the angular scattering of electrons on neutral atoms within an extended energy range. In numerical simulations, the scattering process should adequately reproduce the macroscopic transport properties and also allow rapid sampling of the probability distribution. This problem is well studied, in application to gases[1,2] and also to condensed matter.[3,4] The most important condition for the approximated differential cross-section is that it should yield the correct value of the first transport (momentum-transfer) cross section as a function of electron energy. It should also allow for efficient sampling of the cumulative probability distribution in the Monte Carlo algorithm. An approximation based on screened-Coulomb scattering (also known as Wentzel[5] approximation) with energy-dependent screening can be utilized to match the reference cross-section data provided by experiment and/or accurate theory, and its integrated probability distribution is easy to invert.

We present an accurate practical approximation of energy-dependent screening in helium which is valid for energies between 0.01 and 1000 eV and has correct asymptotic behavior at high energies.

II. WENTZEL APPROXIMATION AND THE ENERGY-DEPENDENT SCREENING PARAMETER FOR ELECTRON SCATTERING IN HELIUM

The differential scattering cross-section of an electron on the potential

$$\phi(r) = V_0 \frac{a}{r} e^{-r/a} \tag{1}$$

in the Born approximation[6] is

$$\frac{d\sigma}{d\Omega} = 4a^2 \left(\frac{V_0 a^2 m}{\hbar^2}\right)^2 \frac{1}{\left[1 + \left(2\frac{mva}{\hbar}\sin\frac{\theta}{2}\right)^2\right]^2}. \tag{2}$$

Here $d\Omega = 2\pi\sin\theta d\theta$ is the element of the spherical scattering angle.

One can formally allow[1,3,4] the screening length a in Eq. (1) to depend on the electron energy E, with the purpose of using the choice of $a(E)$ to approximate a more complicated scattering and not necessarily under the Born conditions. It is convenient to parameterize the screening as follows:[2]

$$\frac{1}{\sigma(E)}\frac{d\sigma}{d\Omega} = \frac{1}{4\pi}\frac{1-\xi^2(E)}{[1-\xi(E)\cos\theta]^2} \tag{3}$$

(with $\xi(E)$ yet to be determined), where E is the energy of the electron, σ is the total cross-section, and θ is the scattering angle. The angle θ is sampled in simulations by inverting the corresponding cumulative probability function

$$\cos\theta = 1 - \frac{2R(1-\xi)}{1+\xi(1-2R)}, \tag{4}$$

with R sampled from a uniform distribution on [0:1]. The function $\xi(E)$, whose values lie between -1 and 1, can be determined from experimental or theoretical data for the transport cross-section

$$\sigma_t(E) = \int_0^\pi (1-\cos\theta)\frac{d\sigma}{d\Omega} 2\pi\sin\theta d\theta. \tag{5}$$

For example, in the particular case of Born cross-section (2), we have $\xi(E) = 1/(1+1/\varepsilon)$, and the scattering angle would be sampled as

$$\cos\theta = 1 - \frac{2R\varepsilon}{2(1-R)+\varepsilon},$$

where $\varepsilon = 4Ema^2/\hbar^2$.

Substituting Eq. (3) into Eq. (5) yields an implicit relation[2] for $\xi(E)$

$$\frac{\sigma_t(E)}{\sigma(E)} = \frac{1-\xi}{2\xi^2}\left((1+\xi)\ln\frac{1+\xi}{1-\xi} - 2\xi\right). \tag{6}$$

For helium gas in the range $0 < E < 1$ keV, based on the published cross-section data,[7] we found a two-pole rational approximation for the screening function $\xi(E)$

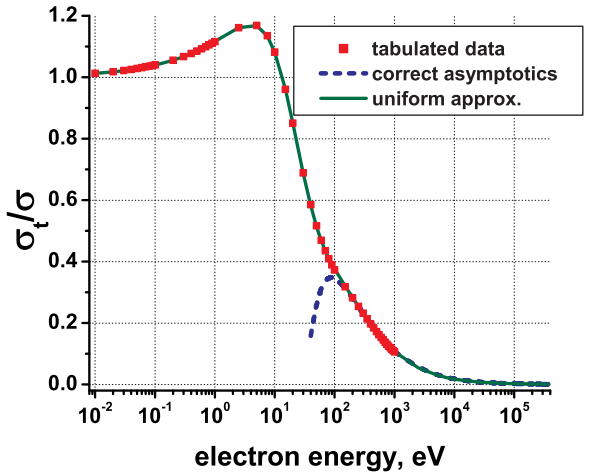

FIG. 1. Comparison of the ratio $\sigma_t(E)/\sigma(E)$ for reference data[7] and for Eqs. (6) and (7) in the range $10^{-2}\,\text{eV} < E < 10^3\,\text{eV}$. Also shown is the required asymptotics given by Eq. (11). In its range of validity $E > 150\,\text{eV}$, it coincides with the present approximation within the plotting accuracy.

$$\xi(E) = 1 + \frac{p_1\sqrt{x} - p_2^2 - p_3}{\left(\sqrt{x} - p_2\right)^2 + p_3} - \frac{p_1\sqrt{x}}{\left(\sqrt{x} - p_4\right)^2 + p_5}, \qquad (7)$$

where $x = E/(1\,\text{eV})$ and

$$p_1 = 2.45,\ p_2 = 2.82,\ p_3 = 11.98,\ p_4 = 5.11,\ p_5 = 64.01.$$

Figure 1 shows a comparison of the approximated ratio σ_t/σ to the one evaluated from the reference data.[7] The relative error in the value of the transport cross-section resulting from Eq. (6) is no higher than 1% within the fitting range $0 < E < 1\,\text{keV}$.

It is important to verify that the approximation for the scattering cross-section given by Eqs. (3) and (7) reproduces the asymptotic behavior of the scattering cross-section at high electron energies, $mva \gg \hbar$, where a is the size of the He atom, which is on the order of the Bohr radius a_0.[6] Under the Born approximation, the elastic differential cross-section is[6]

$$\frac{d\sigma}{d\Omega} = \frac{4m^2e^4}{\hbar^4 q^4}[Z - F(q)]^2, \qquad (8)$$

where $Z = 2$ is the He nucleus charge, $q = 2(mv/\hbar)\sin(\theta/2)$, and $F(q)$ is the form factor. In the limit $qa = 2(mva/\hbar)\sin(\theta/2) \gg 1$, $F(q) \ll 1$ (that is, the electrons in the helium atom do not contribute to scattering) and the scattering cross section is given by the Rutherford formula

$$\frac{d\sigma}{d\Omega} = \left(\frac{Ze^2}{2mv^2}\right)^2 \frac{1}{\sin^4(\theta/2)}. \qquad (9)$$

The total[8,9] and transport[10] cross sections in the limit $mva \gg \hbar$ are given by

$$\sigma(E) \approx \frac{48\,\text{eV}}{E}\pi a_0^2, \qquad (10)$$

$$\frac{\sigma_t(E)}{\sigma(E)} \approx \frac{31\,\text{eV}}{E}[\ln(E/12\,\text{eV}) - 1]. \qquad (11)$$

Making use of Eqs. (3) and (11) shows that in the limit $E \gg 30\,\text{eV}$, the screening function $\xi(E)$ should follow the asymptotic behavior

$$\xi(E) \approx 1 - \frac{31\,\text{eV}}{E}. \qquad (12)$$

This asypmtotics is indeed very closely matched by the two-pole approximation (7). According to Ref. 10, the asymptotic expression for the ratio of the transport and total cross sections given by Eq. (11) is valid with high accuracy (within several per cent) for $E > 150\,\text{eV}$ in the case of helium. Thus, it can be used for determining the screening function $\xi(E)$ for high electron energies $E > 1\,\text{keV}$, where the detailed measurements of differential cross-sections are scarce. We have verified that the accuracy of our two-pole approximation as compared with Eq. (11) is uniformly better than 2% for all (non-relativistic) energies up to 100 keV. At higher energies, relativistic corrections have to be accounted for.

III. COMPARISON OF THE DEVELOPED APPROXIMATION WITH REFERENCE DATA AND ANOTHER APPROXIMATION

In numerical simulations of plasmas utilizing Monte Carlo treatment of electron-neutral collisions, many codes implement an approximation of the differential cross-section in the form

$$\frac{1}{\sigma}\frac{d\sigma}{d\Omega} = \frac{1}{4\pi}\frac{x}{\left(1 + x\sin^2\frac{\theta}{2}\right)\ln(1+x)}, \qquad (13)$$

where $x = E/(1\,\text{eV})$. The cumulative probability distribution is invertible and the scattering angle is sampled according to

$$\cos\theta = 1 + 2\frac{1 - (1+x)^R}{x}, \qquad (14)$$

where R is sampled from a uniform distribution on [0:1]. This *ad hoc* procedure is convenient and computationally efficient. It accounts for the relative increase in scattering

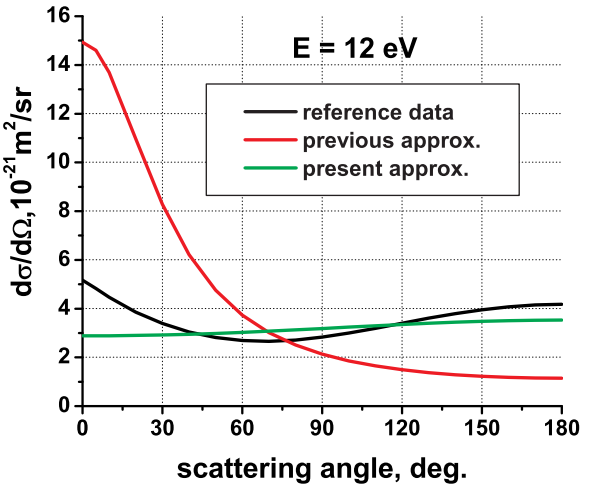

FIG. 2. Comparison of the approximation of the differential cross section given by Eqs. (3), (6), and (7) with the data from Ref. 7 and approximation (13) for electron energy $E = 12\,\text{eV}$.

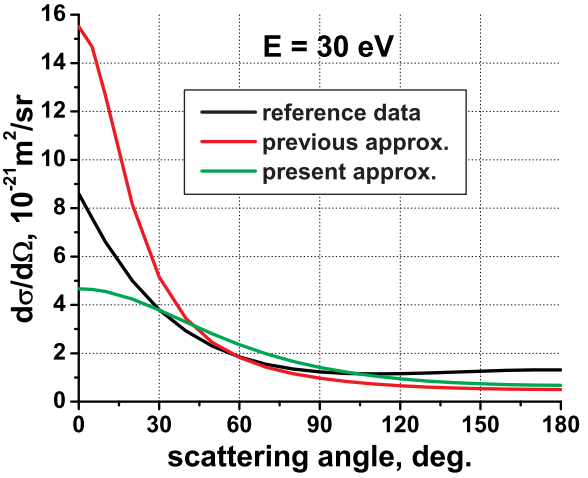

FIG. 3. Comparison of the approximation of the differential cross section given by Eqs. (3), (6), and (7) with the data from Ref. 7 and approximation (13) for electron energy $E = 30$ eV.

into small angles at high electron energy, but does not reproduce other essential physical properties of the differential cross-section. At high energies, the approximation given by Eq. (13) does not reduce to the Rutherford differential scattering cross-section, Eq. (9). In addition, Eq. (13) results in the following ratio of the transport and total cross-sections:

$$\frac{\sigma_t}{\sigma} = 2\frac{1-(1/x)\ln(1+x)}{\ln(1+x)}, \tag{15}$$

which is inaccurate at high electron energies. Instead of the correct $\ln E/E$ asymptotics seen from Eq. (11), Eq. (13) yields $1/\ln E$.

Figures 2–4 show the plots of differential scattering cross-sections given by the two models as well as the actual data.[7] At low energies (<10 eV) in He, the scattering is predominantly backward, and the transport cross-section σ_t exceeds the total cross-section σ due to the $(1-\cos\theta)$ factor in σ_t. For the energy value $E \approx 12$ eV, $\sigma_t \approx \sigma$ and the scattering is nearly isotropic. In contrast, the approximation (13) shows a strong anisotropy. This is because in that model,

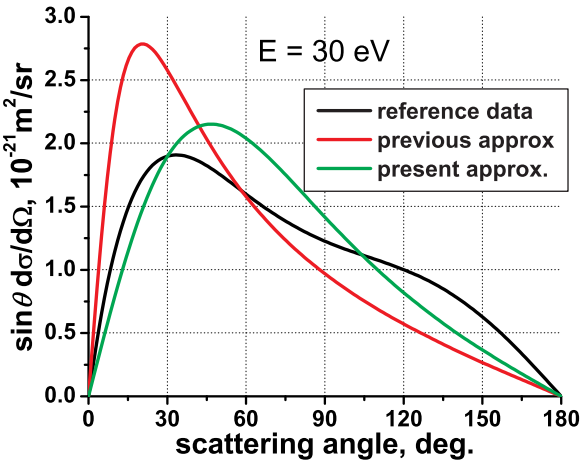

FIG. 4. The same differential cross-section for electron energy $E = 30$ eV as in Fig. 3 but multiplied by $\sin\theta$ to present a quantity proportional to the actual probability density being sampled in MC simulations.

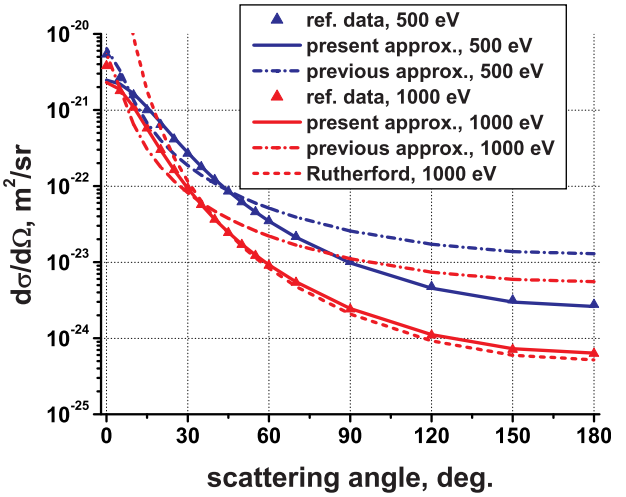

FIG. 5. Comparison of the approximation of the differential cross section given by Eqs. (3), (6), and (7) with the data from Ref. 7 and approximation (13) for electron energies 500 eV and 1000 eV. Note that for angles above 20°, the differential cross section is close to the Rutherford angular dependence given by Eq. (9).

backward scattering is always less frequent than forward scattering. For electron energy $E = 30$ eV, the differential cross-section has a maximum at small scattering angles, see Fig. 3. The proposed screened-Coulomb approximation underestimates the correct value, while the approximation (13) yields an overestimate. At the same time, if one examines the actual probability density which will be sampled in Monte Carlo simulations, namely $\sin\theta d\sigma/d\Omega$ shown in Fig. 4, it is evident that the energy-dependent screening is in better agreement with the data.

The differential scattering cross-sections for higher electron energies of 500 and 1000 eV are shown in Fig. 5.

According to the Born approximation, at not very small angles $2(mva/\hbar)\sin(\theta/2) \gg 1$ which correspond to angles above 20°, the differential scattering cross-sections are given by the Rutherford formula, Eq. (9). From Fig. 5, it is evident that the approximation (13) grossly overestimates large-angle scattering. This property is further illustrated with the help of Fig. 6, showing the ratios of the approximated $d\sigma/d\Omega$ values to those given by the Rutherford formula.

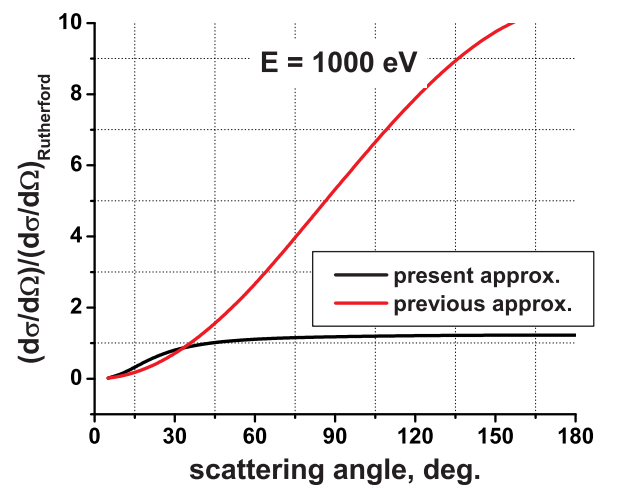

FIG. 6. Ratios of the approximated differential cross sections given by Eqs. (3) and (13) to the Rutherford cross-section (9).

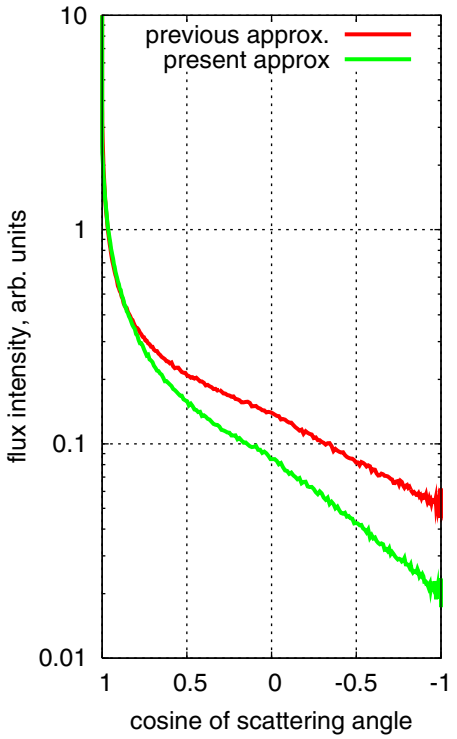

FIG. 7. Angular distributions of the scattered particle flux (flux per unit solid angle Ω) as a function of $\cos\theta = 1 - \Omega/2\pi$, i.e., the flux density distribution, for all electrons in the discharge plasma with energies above 150 eV.

In order to demonstrate the practical difference between two approximations, we performed simulations of a glow discharge in helium. The 1D-3V, particle-in-cell simulations were performed for a short (no positive column) cold-cathode discharge with the gap width 12 mm, discharge voltage 800 V, and gas pressure 3 Torr; the coefficient of ion-electron secondary emission was 0.2. The simulation code was EDIPIC, provided by D. Sydorenko. In the discharge, the electrons are extracted from the cathode due to ion-induced emission and multiply within the cathode fall due to ionization. Electrons with energies above 200 eV undergo only a few large-angle scattering collisions, and their velocity distribution is anisotropic and strongly affected by the details of the differential cross-section. We chose to plot the angular distribution of the particle flux (flux per unit solid angle Ω) as a function of $\cos\theta = 1 - \frac{\Omega}{2\pi}$, i.e., the flux density distribution, for all electrons in the discharge plasma with energies above 150 eV. Figure 7 demonstrates that, as stated above, the approximation (13) overestimates the scattering at high energies and its corresponding angular distribution has a much slower fall-off at large angles compared to the actual scattering process. It therefore yields noticeably higher (2-3 times) flux of energetic electrons undergoing large-angle scattering. In a real physical system, this implies a higher flux of energetic electrons to the side surfaces of the discharge volume, affecting the properties of the corresponding sheaths and the resulting transport properties at the walls.

IV. SUMMARY

We have proposed a procedure for handling elastic collisions of electrons with neutral atoms in helium for Monte Carlo simulations. The implementation involves using Eqs. (4) and (7) within a standard null-collision algorithm or any of its variations. Inelastic collisions are handled in the same manner, which account for the corresponding energy loss.

ACKNOWLEDGMENTS

This research was funded by the U.S. Department of Energy.

[1]P. Belenguer and L. Pitchford, J. Appl. Phys. **86**, 4780 (1999).
[2]A. Okhrimovskyy, A. Bogaerts, and R. Gijbels, Phys. Rev. E **65**, 37402 (2002).
[3]K. Murata, J. Appl. Phys. **45**, 4110 (1974).
[4]J. Fernandez-Varea, R. Mayol, J. Baro, and F. Salvat, Nucl. Instrum. Methods Phys. Res. B **73**, 447 (1993).
[5]G. Wentzel, Z. Phys. **40**, 590 (1927).
[6]L. D. Landau and E. M. Lifshitz, *Quantum Mechanics: Non-Relativistic Theory* (Elsevier, 2003).
[7]M. Adibzadeh and C. Theodosiou, At. Data Nucl. Data Tables **91**, 8 (2005).
[8]M. Inokuti and M. McDowell, J. Phys. B **7**, 2382 (1974).
[9]D. Kennedy, J. Phys. B **1**, 526 (1968).
[10]A. Jablonsky, J. Phys. B **14**, 281 (1981).